Earth Surf. Dynam., 2, 339–348, 2014
www.earth-surf-dynam.net/2/339/2014/
doi:10.5194/esurf-2-339-2014

Earth Surface Dynamics
Open Access

Automated landform classification in a rockfall-prone area, Gunung Kelir, Java

G. Samodra[1,2], G. Chen[2], J. Sartohadi[1], D. S. Hadmoko[1], and K. Kasama[2]

[1]Environmental Geography Department, Universitas Gadjah Mada, Yogyakarta, Indonesia
[2]Graduate School of Civil and Structural Engineering, Kyushu University, Fukuoka, Japan

Correspondence to: G. Samodra (guruh.samodra@gmail.com)

Received: 30 December 2013 – Published in Earth Surf. Dynam. Discuss.: 30 January 2014
Revised: 10 April 2014 – Accepted: 25 April 2014 – Published: 5 June 2014

Abstract. This paper presents an automated landform classification in a rockfall-prone area. Digital terrain models (DTMs) and a geomorphological inventory of rockfall deposits were the basis of landform classification analysis. Several data layers produced solely from DTMs were slope, plan curvature, stream power index, and shape complexity index; whereas layers produced from DTMs and rockfall modeling were velocity and energy. Unsupervised fuzzy *k* means was applied to classify the generic landforms into seven classes: interfluve, convex creep slope, fall face, transportational middle slope, colluvial foot slope, lower slope and channel bed. We draped the generic landforms over DTMs and derived a power-law statistical relationship between the volume of the rockfall deposits and number of events associated with different landforms. Cumulative probability density was adopted to estimate the probability density of rockfall volume in four generic landforms, i.e., fall face, transportational middle slope, colluvial foot slope and lower slope. It shows negative power laws with exponents 0.58, 0.73, 0.68, and 0.64 for fall face, transportational middle slope, colluvial foot slope and lower slope, respectively. Different values of the scaling exponents in each landform reflect that geomorphometry influences the volume statistics of rockfall. The methodology introduced in this paper has possibility to be used for preliminary rockfall risk analyses; it reveals that the potential high risk is located in the transportational middle slope and colluvial foot slope.

1 Introduction

In attempts to study and understand landforms, people have tried to map and document landform features since a long time ago. Summerfield (1991) explained that the first attempts of humans to document landforms started in the age of Herodotus (5th century BC) and Aristotle (384–322 BC). It was described in a simple way. In the early stage of mapping, such features of topography were drawn by the hachure method (Gustavsson, 2005). Nowadays, topography is mapped as contour lines or DTMs (digital terrain models). Topographic maps and DTMs are very important for landform classification and geomorphological mapping.

The landform classification which is based on landform genesis (Verstappen, 1983; van Zuidam, 1983) has been widely used in Indonesia. It is suitable for small-scale geomorphological mapping. However, it is necessary to add the other landform information in order to map geomorphological features in the medium to large scales. In a later development of geomorphological mapping in Indonesia, medium- to large-scale geomorphology maps include the information about relief, parent rock, and geomorphological process.

The detailed geomorphological information is very useful in many fields of study and application. It offers a comprehensive discussion related to another aspect. For instance, the study of hazard analysis will be very beneficial if it is analyzed in the context of geomorphology (Panizza, 1996). Here, geomorphometric analysis can be used as a tool for incorporating disaster risk reduction and transfer measures into development planning. This provides basic ideas for planning priorities in promoting a risk management plan and strategy, and evaluating spatial planning policies. Thus, by using geomorphometry as a preliminary tool for risk

assessment, the spatial planning manager can make a balance between minimizing risk and promoting some development priorities.

Risk can be defined as "the expected number of lives lost, persons injured, damage to property and disruption of economic activity due to a particular damaging phenomenon for a given area and reference period" (Varnes, 1984). The definition was originally used to describe landslide risk. Later, the terminology was used for all types of mass movements including rockfalls.

The word "rockfall" is often distinguished from more general landslide phenomena due to its typical material, size and failure mechanism. It is defined as rock fragments (Hungr and Evans, 1988) with size from a few cubic decimeters to 10^4 m cubic meters (Levy et al., 2011) that detach from their original position (Crosta and Agliardi, 2003) followed by free falling, bouncing, rolling or sliding (Peila et al., 2007). Rockfall risk can be expressed by the simple product of temporal probability, spatial probability, reach probability, vulnerability and value of the element at risk (Fell et al., 2005; van Westen et al., 2005; Agliardi et al., 2009) as follows:

$$R = \sum_{i=1}^{I} \sum_{j=1}^{J} \sum_{k=1}^{K} \sum_{m=1}^{M} P(L)_{jkm} \cdot P(T|L)_{ij} \cdot P(I|T)_i \cdot V_{ij} \cdot E_i, \quad (1)$$

where $P(L)_{jkm}$ is the temporal probability (exceedance probability) of rockfall in the magnitude scenario (i.e., boulder volume) class j and crossing landform k for different period m; $P(T|L)_{ij}$ is the probability of the rockfall in the volume class j reaching the element at risk i; $P(I|T)_i$ is the temporal spatial probability of the element at risk i, V_{ij} is the vulnerability of the element at risk i to the magnitude class j and E_i is the economic value of the element at risk i.

Based on the Eq. (1), the magnitude and exceedance probability of rockfalls are diverse in time and places. The 9-unit slope model (Dalrymple et al., 1968, i.e., interfluves, seepage slope, convex creep slope, fall face, transportational midslope, colluvial foot slope, alluvial foot slope, channel wall and channel bed) can pose important zones of rockfall processes where energy and velocity are diverse in places. It can be delineated into key information for prioritization of mitigation actions. The information is useful to expose the spatial distribution of elements at risk of potentially high damage from rockfalls. Thus, selection of preventive mitigation measure type, structural protection location, and structural protection dimension should be supported by a rockfall risk assessment based on landform analysis.

Traditionally, landform analysis (delineation and classification procedure) is based on the stereoscopic technique of aerial photo and field investigations. This method is very common in Indonesia. It has been applied for soil mapping, land evaluation analysis, land suitability analysis, spatial planning, and so on. It is also mentioned in Indonesia's national standard document of geomorphological mapping that the technical requirement for geomorphological mapping is an interpretation of remote sensing data combined with field measurements (SNI, 2002). The standard landform classification in Indonesia is based on the ITC (International Institute for Geo-Information Science and Earth Observation) classification system (van Zuidam, 1983). However, the traditional method of landform classification requires simultaneous consideration and synthesis of multiple different criteria (MacMillan and Shary, 2009) and the quality depends on the skill of the interpreter. The developed landform classification has been applied mostly in soil landscape studies. Thus, we try to automatically classify landforms based on the 9-unit slope model, which is appropriate to rockfall analysis. Even though, the 9-unit slope model is significant for a pedogeomorphic process–response system (Conacher and Dalrymple, 1977), it is also relevant for preliminary rockfall risk zoning.

2 Study area

Gunung Kelir is located in the Yogyakarta Province, Indonesia. It lies in the upper part of the Menoreh Dome, which is located in the central part of Java Island (Fig. 1). The area is dominated by a tertiary Miocene Jonggrangan Formation that consists of calcareous sandstone and limestone. Bedded limestone and coralline limestone, which form isolated conical hills, may also be found in the highest area surrounding the study area.

Landforms in Gunung Kelir are a product of the final uplifting of the Complex West Progo Dome in the Pleistocene. The evolution or chronology of the Kulon Progo Dome has been well explained by van Bemmelen (1949). It started with the rising up of the geosyncline of southern Java in the Eocene Epoch. It made the magma of the Gadjah Volcano, consisting of basaltic pyroxene andesites, reach up to the surface. Then, it was followed by the activity of the Idjo Volcano in the south with more acid magma consisting of hornblende-augite andesites and dacite intrusions. After the strong denudation process, exposing the chamber of the Gadjah Volcano, the Menoreh Volcano in the north began to be active. The material consists of hornblende-augite andesites and without lava flow ended by dacitic intrusion and hornblende andesite with the doming up process. Then, in the lower Miocene, the Kulon Progo Dome subsided below sea level and the Jonggrangan Formation was formed by coral reef sedimentation. Finally, the complex of The Progo Dome was uplifted during the Pleistocene. The uplifting caused jointing and large cracks and caused abundant rockfalls and slides to the foot of the Kulon Progo Dome especially in its eastern flank.

The terms Gunung and Kelir come from Javanese Language. Gunung can be translated as mountain and Kelir is a curtain that is used to perform wayang (performance with traditional Javanese shadow puppets). Its toponym describes a 100–200 m high escarpment that has a maximum slope of

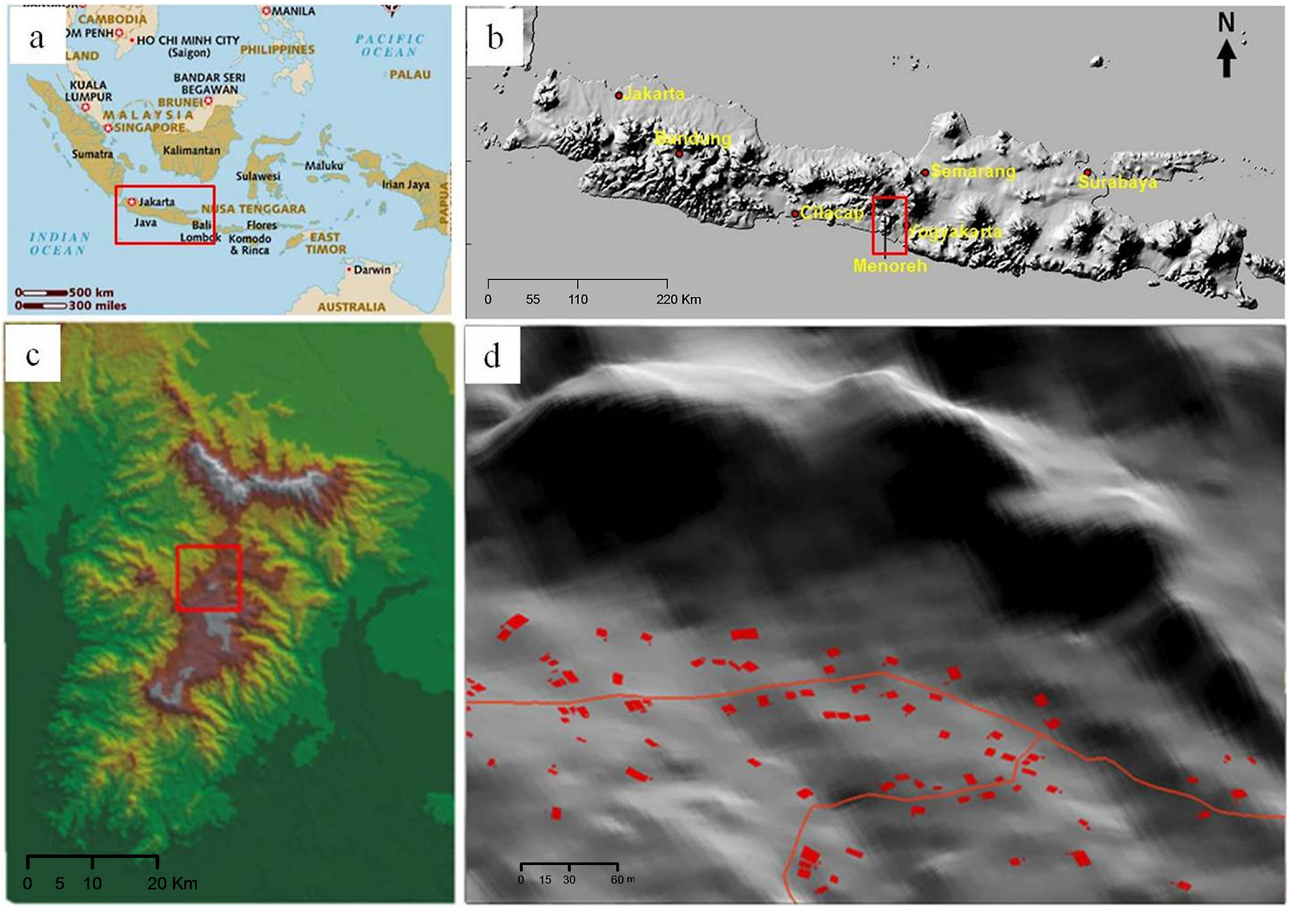

Figure 1. Study area **(a)**, geographical position of Java Island **(b)**, DTM of Java Island **(c)**, DTM of the Kulon Progo Dome **(d)**, Gunung Kelir area viewed from the east: red rectangles are elements at risk.

nearly 80°. The complex of Gunung Kelir consists several generic landforms that are prone to rockfall. Its mean slope gradient is 23.14° with the standard deviation of 13.05°. Altitude ranges from 297.75 to 837.5 m. There are 152 buildings exposed as elements at risk on the lower slope of the escarpment (Fig. 1d).

3 Data and methods

Rockfall risk analysis requires assessment of susceptibility and identification of an element at risk. To portray the susceptible area, geomorphological opinion is commonly used to classify landform through interpretation of aerial photos and field surveys. However, the subjectivity of the investigator hinders the application of this method. Therefore, unsupervised landform classification based on the 9-unit slope model is applied in the present study. The main objective of this study is to provide automated landform classification particularly for rockfall analysis. To achieve the primary objective, several works are conducted in this study: (1) fieldwork, (2) DTM preprocessing, (3) DTM processing, (4) rockfall modeling, (5) landform classification based on fuzzy *k* means, and (6) rockfall volume statistics.

Fieldwork was intended to identify rockfall boulders and elements at risk. A field inventory of fallen rockfall boulders of different size was done to obtain the spatial distribution and dimension of rockfall deposition. The dimension and potential source of rockfalls were determined to simulate rockfall trajectory, velocity, and energy. The buildings on the lower slope of the escarpment were also plotted in order to obtain the spatial distribution of elements at risk. Finally, DGPS (differential global positioning system) profiling was conducted to improve the performance of DTM.

The objective of DTM preprocessing was to improve the quality of DTM-derived products. We applied DTM preprocessing proposed by Hengl et al. (2004) including reduction of padi terraces, reduction of outliers, incorporation of water bodies, and reduction of errors by error propagation. Padi terraces are usually caused by the interpolation method and are located in a closed contour where all the surrounding pixels were assigned the same elevation value. The 5 m resolution of DTM was produced by interpolation, using the ILWIS (Integrated Land and Watershed Management Information

Table 1. Coefficient restitution of surface type.

Surface types	R_N	R_T
Sandstone face	0.53	0.9
Vegetated soil slope	0.28	0.78
Soft soil, some vegetation	0.30	0.3
Limestone face	0.31	0.71
Talus cover with vegetation	0.32	0.8

System) linear interpolation method, from a 1 : 25 000 topographical map of 1999 with a contour interval of 12.5 m and elevation data from DGPS profiling. DTM processing generated several morphometric and hydrological variables such as slope, plan curvature, SPI (stream power index) and SCI (shape complexity index) (Fig. 2). DTM-derived products were processed in ILWIS software with several scripts available in Hengl et al. (2009).

The other morphometric variables were rockfall velocity and energy. These were processed by RockFall Analyst as an extension of ArcGIS (Lan et al., 2007). It included modeling of rockfall trajectory by a kinematic algorithm and raster neighborhood analysis to determine their velocity and energy of rockfalls. Rockfall velocity and energy analyses are needed information about slope geometry and other parameters such as mass, initial velocity, coefficient of restitution, friction angle and minimum velocity offset. There were two coefficients of restitution, i.e., normal restitution (R_N) and tangential restitution (R_T), employed in the model (Table 1). Normal restitution acts in a direction perpendicular to the slope surface and tangential restitution acts in a direction parallel to the surface during each impact of the incoming velocity of the rocks. Velocities change because of the energy loss defined by both. We determined normal restitution and tangential restitution with a geological map presenting elasticity of the surface material and a land use map presenting vegetation cover and surface roughness, respectively. Slope geometry was derived from a corrected DTM. The other parameters were derived from secondary data and field data. For example, the coefficient friction angle was derived from a literature review and mass was determined from the dimension of boulders derived from field measurements data.

The landform elements were derived, as the 9-unit slope model, by using the unsupervised fuzzy k means classification (Burrough et al., 2000) as

$$\mu_{ic} = \frac{\left[(\mathrm{d}_{ic})^2\right]^{-1/(q-1)}}{\sum_{c'=1}^{k}\left[(\mathrm{d}_{ic})^2\right]^{-1/(q-1)}}, \quad (2)$$

where μ is the membership of ith object to the cth cluster, d is the distance function, which is used to measure the similarity or dissimilarity between two individual observations, and q is the amount of fuzziness or overlap ($q = 1.5$). Supervised k means classification was written and applied in ILWIS script with an additional class center for each morphometric variable (Table 2). The 9-unit slope model was modified by excluding the alluvial toe slope and seepage slope for the final landform classification. Channel wall was also modified as lower slope. Since the study area is located in the upper part of the Kulon Progo Dome, the depositional process of alluvium does not work in such an area. Seepage slope was merged with interfluves because both are more related to a pedogeomorphic process rather than a gravitational process.

The observed volume of rockfall and cumulative distribution in four generic landforms were plotted in a log–log chart. Hungr et al. (1999) and Dussauge et al. (2003) investigated the frequency–volume distribution of rockfalls. They found that rockfall volumes follow a power-law distribution with relatively similar exponent value. The observed cumulative volume distribution was adjusted by a power-law distribution as follows:

$$N_R = rV_R^{-b}, \quad (3)$$

where N_R is the number of events greater than V_R, V_R is the rockfall volume and b is a constant parameter (cumulative power-law scaling exponent). Linear regression was adopted to estimate the b value.

Similarly to Eq. (3), Dussauge et al. (2003) and Malamud et al. (2004) show that magnitude–frequency distribution of rockfall events in a given volume class j followed a power-law distribution and can be described as

$$\mathrm{Log}N(V) = N_0 + b\log V, \quad (4)$$

where $N(V)$ is the cumulative annual frequency of rockfall events exceeding a given volume V, N_0 is the total annual number of rockfall events, and b is the power-law exponent.

4 Results and discussion

4.1 Landform classification

Geomorphometry defined as quantitative landform analysis (Pike et al., 2008) was initially applied for the assessment and mitigation of natural hazards (Pike, 1988). Van Dijke and van Westen (1990), for example, introduced rockfall hazard assessment based on geomorphological analysis. Later, Iwahashi et al. (2001) analyzed slope movements based on landform analysis. Both utilized DTMs derived from interpolation of 1 : 25 000 contour maps to analyze the geomorphological hazard. Nowadays, the interpolation of contour maps is still useful to create medium-scale mapping when better resolution DTMs are not available. However, the reduction of error in interpolation of contour mapping is needed to obtain a plausible geomorphological feature.

The result of DTM preprocessing shows that padi terraces still exist where the sampling points of elevation data are unavailable. In addition, "flattening" topography can also be found on slopes of less than 2 %. The remaining padi terraces

Table 2. Class centers for each morphometric variable (SD, standard deviation; PlanC, plan curvature; SPI, stream power index; SCI, shape complexity index).

Landforms	Slope (%)	PlanC	SPI	SCI	Energy (kJ)	Velocity ($m\,s^{-1}$)
Interfluve	0	0	1.0	0	0	0
Convex creep slope	6.0	5.0	3.0	5.0	0.5	0.2
Fall face	40.0	−2.0	50.0	5.5	800.0	20.0
Transportational mid. slope	10.0	−1.0	30.0	7.2	1800.0	30.0
Colluvial foot slope	4.0	2.0	15.0	5.0	400.0	10.0
Lower slope	5.0	2.0	75.0	5.0	0	0
Channel bed	5.0	−5.0	400.0	3.0	0	0
SD/variation	5.79	4.30	158.1	1.4	138.9	3.0

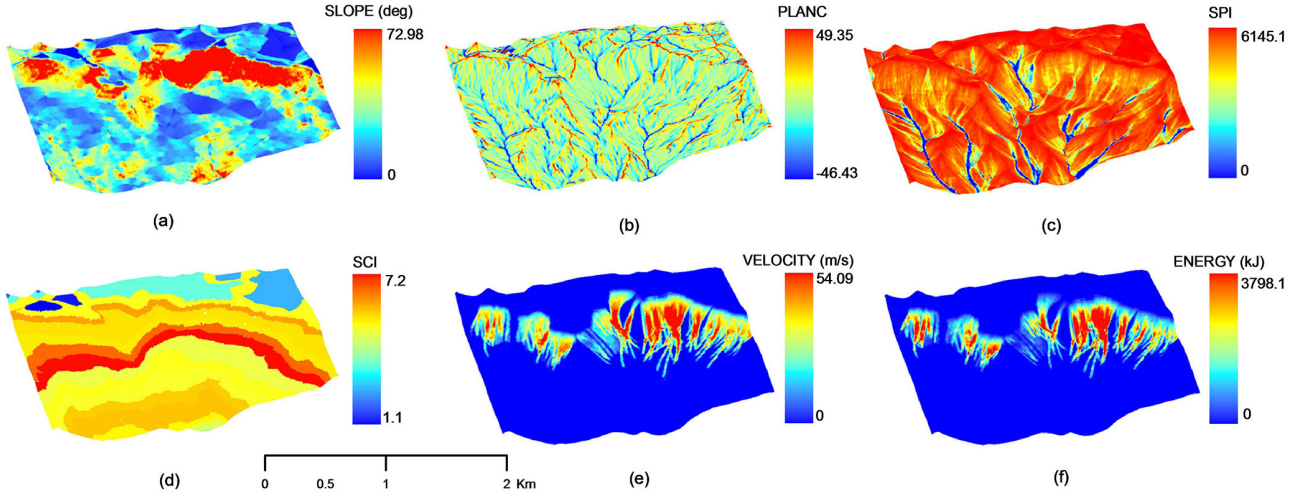

Figure 2. Morphometric variables: **(a)** slope, **(b)** plan curvature, **(c)** stream power index, **(d)** shape complexity index, **(e)** rockfall velocity, and **(f)** rockfall energy.

mostly occur in the transportational middle slope and the flattening phenomenon mostly occurs in the interfluves. Both errors influence the plausibility of slope (Fig. 2a), but do not influence much the final classification of landform elements.

Prior to data analysis, a fundamental decision should be made in relation to the number of landform class and the selection of morphometric variables to be used. The final classification of landform elements should represent an appropriate semantic description related to rockfall processes. A modified 9-slope model was used to represent conceptual entities of rockfall deposition in each slope segment. Convex creep slopes represent a potential rockfall source. Considering that its position is adjacent to a fall face, convex creep slopes and the upper part of fall face are the most likely rockfall sources. A big boulder, which eventually falls, could be part of a convex creep slope and part of a fall face. A fall face represents the Gunung Kelir escarpment, which is dominated by slope > 60° and falling processes. Velocity increases significantly in the fall face and reaches a maximum in the transportational middle slope. In the transportational middle slope, velocity starts to decrease during the contact between boulder and surface. Bouncing, rolling and sliding are dominant in a transportational middle slope. Some high-velocity and high-energy boulders may continue their movement to a colluvial foot slope. This depends on the local surface and the presence of an obstacle that can stop the movement of boulders.

When selecting morphometric variables one should also consider rockfall processes, besides morphology of the landscape. They should reflect the movement and deposition of rockfall boulders. Prior to the selection of morphometric variables, knowledge of rockfall processes in relation to generic landforms should be utilized. Experience and former knowledge are involved during the selection of morphometric variables.

Derivation of morphometric variables through DTM processing was divided into two parts, i.e., morphometric variables derived from RockFall analyst (velocity, energy) and from the ILWIS script (slope, plan curvature, shape complexity index, stream power index). Rockfall velocity and energy are secondary derivatives of a DTM (Lan et al., 2007). The first derivatives (i.e., slope angle and aspect angle) were

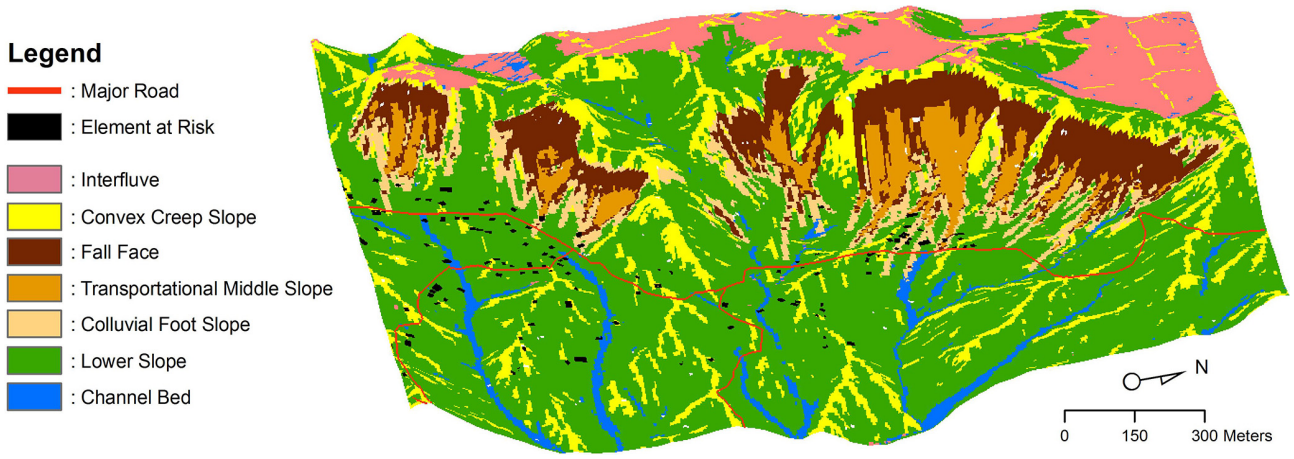

Figure 3. Generic landforms in Gunung Kelir.

employed to compute the rockfall trajectory. Then, rockfall trajectory was used to model the rockfall velocity and rockfall energy by using neighborhood and geostatistical analysis. Velocity and energy of rockfall, as a result of gravitational slope phenomena, may be spatially correlated. Those which are closer tend to be more alike than those that are farther apart. The spatial autocorrelation can be performed with geostatistical techniques.

The highest velocity occurs in the transportational middle slope. Velocity gradually increases in the fall face and decreases in the colluvial foot slope. Since the energy is also calculated from rockfall velocity, the spatial distribution pattern of energy is very similar to the rockfall velocity. Both velocity and energy of rockfall are mostly influenced by slope geometry, coefficient of restitution, and friction angle. The first change of a pixel into zero velocity and energy of its neighborhood operation is determined at the end of boulder movements, meaning that the rockfall boulders are deposited on this site.

Plan curvature and stream power index influence the pattern of the convex creep slope and the channel bed. Shape complexity index, sliced using an equal interval of 25 m, was measured as the outline complexity of a 2-D object. It was calculated using the perimeter to boundary ratio of the sliced feature. SCI indicates how oval a feature is. A low value of SCI represents how simple and compact a feature is. SCI predominantly influences the spatial distribution of the interfluves, which have a low value of around 1, meaning that interfluves are more oval, while convex creep slope and fall face are more longitudinal. Its effect on the other landforms is not apparent because the value of the shape complexity index in the lower slope is relatively homogeneous, i.e., 4–5.

The generic landform result will depend on how well morphometric variables are selected to perform automated landform classification. It represents how well a morphometric variable can describe the specific process working on a landform element. Its spatial dependency influences the application of automated landform mapping in different places and different geomorphological process.

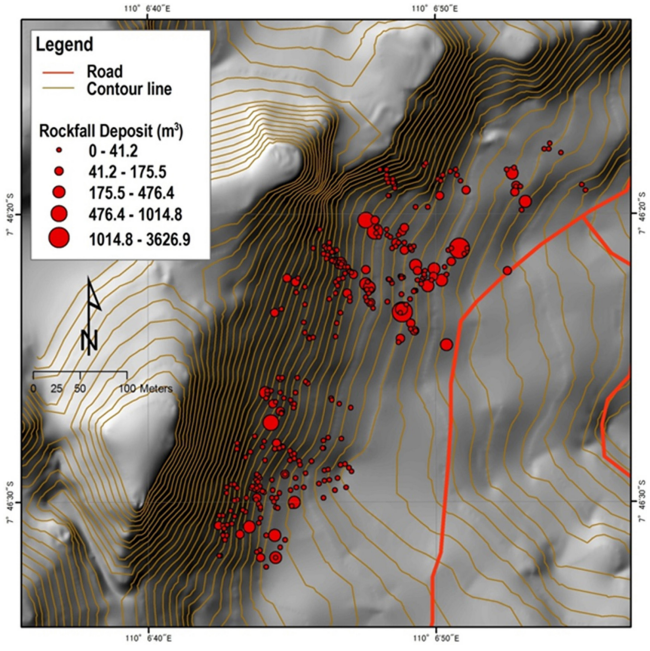

Figure 4. Distribution of rockfall boulders in Gunung Kelir obtained from geomorphological survey.

The final classification result (Fig. 3) was draped over a DTM. The volume of statistical rockfall deposits was employed to evaluate the coincidence between landform classification and rockfall frequency–magnitude. Since landform classification considers surface form and process, we argue that landform classification in a rockfall-prone area exhibits scale-specificity (Evans, 2003). The magnitude (volume) and frequency of boulder deposits may have a specific scale related to each generic landform.

Table 3. Characteristic of rockfall volume distribution in Gunung Kelir.

Generic landform	Area, km^2	N_{events}	V_{total}, m^3	V_{range}, m^3	V_{fit}, m^3	N_{fit}	b_{lr}	R^2	Error margin*
Fall face	0.11	53	513.49	18×10^{-4}–1.0×10^{2}	2–1.0×10^{2}	28	0.58	0.98	0.046
Transportational middle slope	0.06	211	9627.59	39×10^{-4}–3.6×10^{3}	11–3.6×10^{3}	63	0.73	0.99	0.022
Colluvial foot slope	0.1	199	6287.16	37×10^{-4}–4.8×10^{2}	10.5–4.8×10^{2}	70	0.68	0.99	0.019
Lower slope	4.18	58	5004.30	21×10^{-4}–3.6×10^{3}	11–3.6×10^{3}	21	0.64	0.97	0.071

* Assumes a 95 % level of confidence.

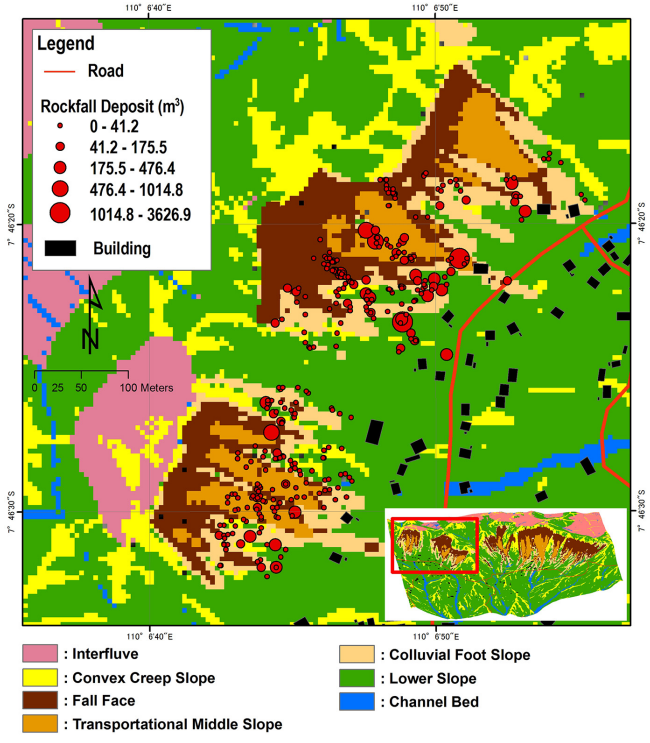

Figure 5. Distribution of rockfall boulders associated with elements at risk and generic landforms.

4.2 Rockfall statistics and landform

The 521 rockfall deposits in our geomorphological inventory range in size from 18×10^{-4} to 3.6×10^{3} (Fig. 4). Those are deposited spatially in four main landforms, i.e., fall face, transportational middle slope, colluvial foot slope and lower slope (Fig. 5). Rockfalls deposited on the fall face are mostly found in the southern part of the Gunung Kelir area. There are 47 rockfall boulders in the southern part. The southern fall face has a gentler slope and softer rock than the northern part. Gully erosion can be found in this place due to weathering and erosion. Small volumes of rockfall are mostly deposited in gullies; those are stopped and trapped due to local surface affected by weathering and erosion. However, 12.5 m contours cannot draw this phenomenon. A better resolution of DTMs may be useful to show gully erosion.

The rockfall statistics observed based on the main landforms corresponding to rockfall deposition, i.e., fall face, transportational middle slope, colluvial foot slope and lower slope, indicate that the observed distributions for 53, 211, 199, and 58 events larger than 2, 11, 10, and 11 m^3 are well fitted by power laws with b of 0.58, 0.73, 0.68, and 0.64, respectively. The power-law distribution is well fitted to explain 55, 30, 36 and 38 % of the boulder deposits population in the fall face, transportational middle slope, colluvial foot slope and lower slope, respectively. The model is not well fitted to explain small size rockfall deposits due to the rollover phenomenon. It needs many reports obtained from complete historical rockfall data in many places with different physical characteristics to obtain "general" agreement in assessing rockfall distribution. In many places, such complete historical data are absent.

However, several authors agreed that volume distribution of rockfall follows a power-law distribution. There is still lack knowledge of the b value due to the absence of complete inventory data. Dussauge et al. (2003) argue that the variation of the b value is due to the variability of cliff dimension, area scale, lithology, geometrical and mechanical parameters of rockfalls. Hungr et al. (1999) proposed that jointed rock ($b = 0.65$–0.70) has a higher b value than massive rock ($b = 0.40$–0.43). Gunung Kelir is a subvertical cliff dominated by calcareous limestone. It has $b = 0.58$–0.73 for a volume larger than 2 and 10 m^3. It shows that this study may also confirm the b value for jointed rock proposed by Hungr et al. (1999). Lithology and surface material play important roles for rockfall volume distribution; they influence the bouncing velocity during the impact between rockfall boulder and surface material. Soft rock tends to reduce the energy and decrease the velocity of rockfall.

Landform also influences the value of a scaling exponent. Fall face has the smallest b value, which also indicates that lower frequency of smaller events is more dominant in the fall face. Whereas, higher frequency of greater events is more dominant in the transportational middle slope and colluvial foot slope, which shows the gradation pattern of rockfall deposition around generic landforms. This may correspond to the morphometric condition. The shape and characteristics of the surface, i.e., morphometric variables, determine how a rockfall was deposited. Initially, we considered that the distribution pattern along the x axis and y axis was influenced

by the number of measurements in the rockfall boulder data sets in each landform. The distribution pattern of the fall face seems similar to the lower slope while the transportational middle slope is similar to the colluvial foot slope (Table 3). However, the trend only occurs in the volumes < 2 m^3 for the fall face and lower slope, and < 80 m^3 for the transportational middle slope and colluvial foot slope. As stated by Brunetti et al. (2008), we also consider that the distribution pattern is not influenced by the number of measurements in the data set.

All landforms exhibit a rollover of the frequency of rockfall boulders. It is similar to the rollover identified by Dussauge et al. (2003), Hungr et al. (1999), and Guthrie et al. (2004). Roll over occurs in the volume size of around 3 m^3 for the fall face, 11 m^3 for lower slope, and 6 m^3 for colluvial foot slope and transportational middle slope. Since the rockfall process is more related to the deposition zone rather than failure zone, a "rollover" to frequencies should be addressed to the process during the impact between rockfall boulder and surface. The rockfall boulders were deposited on the site when the local surface decreased the volume and energy to zero velocity. This can be influenced by a soft surface condition and or an obstacle that can interfere with the movement of a boulder.

The gradation pattern of rockfall deposition may be addressed to scale specificity (Evans, 2003). The volume of the individual rockfall deposit in the fall face spans 5 orders of magnitude. The landforms that have higher orders of magnitude are lower slope, colluvial slope and transportational middle slope, respectively. Careful attention should be addressed to the maximum individual boulder deposited in the lower slope. Figure 6 shows that the volume of rockfall deposits in the lower slope spans 6 orders magnitude. However, it indicates a long missing gap between the largest boulder (3626.97 m^3) and the second largest boulder (372.84 m^3). The local surface parameter may influence this problem. We consider that the maximum order magnitude on the lower slope is rather similar with the colluvial foot slope (around 400 m^3). The likelihood for the deposition of greater rockfall volume can be defined. The higher magnitude of rockfall is more likely to be deposited on the transportational middle slope rather than on the colluvial foot slope, transportational middle slope or lower slope. This information is important for rockfall risk analyses.

4.3 Implication for preliminary rockfall risk analysis

In the past, many people used to consider that natural hazards should be approached from the engineering fields. However, both structural and nonstructural mitigation should be included in natural hazard mitigation comprising geomorphological, geographical, and geological approaches (Oya, 2001). Specific geomorphology features may pose a specific hazard. The most susceptible places, in order, for rockfall susceptibility in the Gunung Kelir area are the fall face,

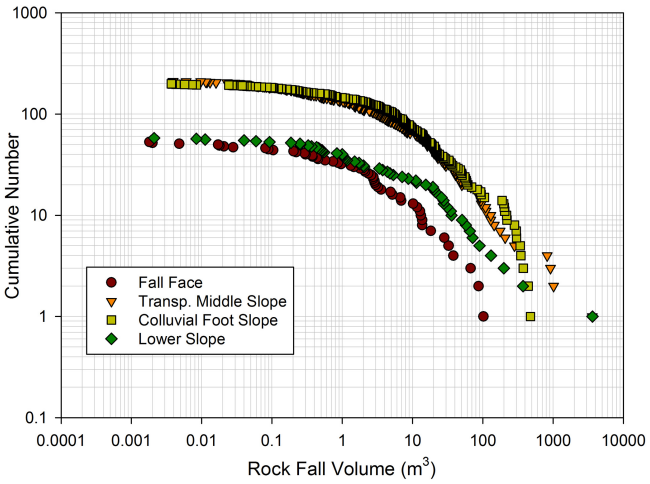

Figure 6. Cumulative frequency curves of rockfall volume.

transportational middle slope, colluvial foot slope and lower slope, respectively, each of which exhibits scale specificity.

Automated landform analysis and rockfall statistics can estimate the likelihood of rockfall magnitude in a specific landform. Each generic landform indicates its degree of susceptibility to rockfall events. The magnitude–frequency relation of rockfalls can be calculated to estimate the annual frequency of rockfall events in each generic landform. It can be defined with reference to specific event magnitude class in a specific generic landform

Preliminary rockfall analysis can be delivered by evaluating elements at risk located in the place susceptible to rockfall hazards. There are 3 buildings located on the transportational middle slope and 14 buildings located on the colluvial foot slope. This is useful information on which to base prioritization action for countermeasure policies and design. Geomorphologic analysis should be taken into account to locate structural measures (e.g., barriers, embankments, rock sheds) in suitable locations. It will improve cost efficiency by optimizing budget and design. The information of buildings located on landforms classified with a high hazard can also be an input to the prioritization of an evacuation procedure. Therefore, the prioritization of mitigation action based on geomorphometric analysis can meet the technical suitability and the effectiveness of selected mitigation options.

5 Conclusions

The application of geomorphometry can be an alternative tool to minimize the subjectivity of Indonesia's standard landform classification applied in disaster risk reduction. Our models explain 55, 30, 36 and 38 % of the boulder deposits population. Rockfall protection through structural measures and land use planning should take into account landform analysis.

However, the original classification of 9-unit slope model should be modified if it is applied in different places. It should consider the origin's effect on the specific landforms. The final classification of landform elements, i.e., interfluves, convex creep slope, fall face, transportational middle slope, colluvial foot slope, slope and channel bed, is different with the original classification of the 9-unit slope model. The considerations to merge and exclude some landforms were based on the experience and the judgement of researchers. The proposed methodology applied in the rockfall-prone area should be tested in different areas that have a similar genesis. Further studies should also explain the effects of scale and spatial dependency on the landform classification.

Acknowledgements. The authors are very grateful to Ian Evans, Tomislav Hengl, and an anonymous reviewer for their detailed and constructive review. We also thank to our colleagues in the Environmental Geography Department, Universitas Gadjah Mada, for their support in conducting the field survey.

Edited by: T. Hengl

References

Agliardi, F., Crosta, G. B., and Frattini, P.: Integrating rockfall risk assessment and countermeasure design by 3D modelling techniques, Nat. Hazards Earth Syst. Sci., 9, 1059–1073, doi:10.5194/nhess-9-1059-2009, 2009.

Burrough, P. A., van Gaans, P. F. M., and MacMillan, R. A.: High resolution landform classification using fuzzy *k* means, Fuzzy Sets Syst. , 113, 37–52, 2000.

Conacher, A. J. and Dalrymple, J. B.: The nine unit land surface model: an approach to pedogeomorphic research, Geoderma, 18, 1–154, 1977.

Crosta, G. B. and Agliardi, F.: A methodology for physically based rockfall hazard assessment, Nat. Hazards Earth Syst. Sci., 3, 407–422, doi:10.5194/nhess-3-407-2003, 2003.

Dalrymple, J. B., Blong, R. J., and Conacher, A. J.: A hypothetical nine unit landsurface model, Zeitschrift für Geomorphologie, 12, 60–76, 1968.

Dussauge, C., Grasso, J., and Helmstetter, A.: Statistical analysis of rockfall volume distributions: implications for rockfall dynamics, J. Geophys. Res., 108, 2286, doi:10.1029/2001JB000650, 2003.

Evans, I. S.: scale specific landforms and aspects of the land surface, in: concepts and modelling in geomorphology: international perspective, edited by: Evans, I. S., Dikau, R., Tokunaga, E., Ohmori, H., Hirano, M., TERRAPUB, Tokyo, 61–84, 2003.

Fell, R., Ho, K. K. S., Lacasse, S., and Leroi, E. A: framework for landslide risk assessment and management, in: Landslide Risk Management, edited by: Hungr, O., Fell, R., Couture, R., Eberhardt, E., Taylor and Francis, London, 3–26, 2005.

Guthrie, R. H. and Evans, S. G.: Analysis of landslide frequencies and characteristics in a natural system, Coastal British Columbia, Earth Surf. Proc. Land., 29, 1321–1339, 2004.

Hengl, T., Gruber, S., and Shrestha, D. P.: Reduction of errors in digital terrain parameters used in soil–landscape modelling, Internat. J. Appl. Earth Observat. Geoinform., 5, 97–112, 2004.

Hengl, T., Maathuis, B. H. P., and Wang, L.: Geomorphometry in ILWIS, in: Geomorphometry: concepts, software, applications, edited by: Hengl, T. and Reuter, H. I., Developments in soil science, Elsevier, Amsterdam, vol. 33, 497–525, 2009.

Hungr, O. and Evans, S. G.: Engineering evaluation of fragmental rockfall hazards, Proceedings 5th International Symposium on Landslides, Lausanne, Switzerland, 1, 685–690, 1988.

Hungr, O., Evans, S. G., and Hazzard, J.: Magnitude and frequency of rock falls and rock slides along the main transportation corridors of southwestern British Columbia, Can. Geotech. J., 36, 224–238, 1999.

Iwahashi, J. and Pike, R. J.: Automated classifications of topography from DEMs by an unsupervised nested-means algorithm and a three-part geometric signature, Geomorphology, 86, 409–440, 2007.

Lan, H., Martin, C. D., and Lim, C. H.: RockFall analyst: a GIS extension for three-dimensional and spatially distributed rockfall hazard modelling, Comput. Geosci., 33, 262–279, 2007.

Levy, C., Jongmans, D., and Baillet, L.: Analysis of seismic signals recorded on a prone-to-fall rock column (Vercors massif, French Alps), Geophys. J. Internat., 186, 296–310, 2011.

MacMillan, R. A. and Shary, P. A.: Landforms and landform elements in geomorphometry, in: Geomorphometry: Concepts, Software, Applications, edited by: Hengl, T. and Reuter, H. I., Developments in Soil Science, Elsevier, Amsterdam, vol. 33, 227–254, 2009.

Malamud, B. D., Turcotte, D. L., Guzzetti, F., and Reichenbach, P.: Landslide inventories and their statistical properties, Earth Surf. Proc. Land., 29, 687–711, 2004.

Oya, M.: Applied geomorphology for mitigation of natural hazard. Kluwer Academic Publisher, Dordrecht, the Netherlands, 2001.

Panizza, M.: Environmental geomorphology, Elsevier, Amsterdam, the Netherlands, 1996.

Peila, D., Oggeri, C., and Castiglia, C.: Ground reinforced embankments for rockfall protection: design and evaluation of full scale tests, Landslides, 4, 255–265, 2007.

Pike, R. J.: The geometric signature: quantifying landslide-terrain types from Digital Elevation Models, Mathemat. Geol., 20, 491–511, 1988.

Pike, R. J., Evans, I., and Hengl, T.: Geomorphometry: a brief guide, in: Geomorphometry: concepts, software, applications, edited by: Hengl, T. and Reuter, H. I., Developments in soil science, Elsevier, Amsterdam, 3–30, vol. 33, 2008.

SNI: Standar Nasional Indonesia (Indonesia National Standard), Penyusunan peta geomorfologi (geomorphology mapping), Badan Standarisasi Nasional, 2002.

Summerfield, M. A.: Global geomorphology, Addison Wesley Longman Limited, Harlow, Essex, England, 1991.

van Bemmelen, R. W.: The geology of indonesia, Vol. II, Government Printing Office the Hague, 1949.

van Dijke, J. J. and van Westen, C. J.: Rockfall hazard: a geomorphologic application of neighbourhood analysis with Ilwi, ITC Journal, 1, 40–44, 1990.

van Westen, C. J., Asch van, T. W. J., and Soeters, R.: Landslide hazard and risk zonation-why is it still so difficult?, Bull. Eng. Geol. Env., 65, 167–184, doi:10.1007/s10064-005-0023-0, 2005

van Zuidam, R. A.: Guide to geomorphological aerial photographic interpretation and mapping, ITC, Enschede, the Netherlands, 1983.

Varnes, D. J.: Landslide hazard zonation: a review of principles and practice, United Nations Educational, Scientific and Cultural Organization (UNESCO), Paris, 1984.

Verstappen, H. T.: Applied geomorphology, Elsevier Science Publisher Co., Amsterdam, 1983.